Signal Processing 204 (2023) 108836

Contents lists available at ScienceDirect

Signal Processing

journal homepage: www.elsevier.com/locate/sigpro

A novel parametrization of α-spline functions: Application to digital filter design

Miguel Ángel Raposo–Sánchez[a,*], José Sáez–Landete[b], Fernando Cruz–Roldán[b]

[a] Department of Física y Matemáticas (EPS), Universidad de Alcalá, Alcalá de Henares (Madrid) 28805, Spain
[b] Department of Signal Theory and Communications (EPS), Universidad de Alcalá, Alcalá de Henares (Madrid) 28805, Spain

ARTICLE INFO

Article history:
Received 4 June 2021
Revised 14 October 2022
Accepted 1 November 2022
Available online 3 November 2022

Keywords:
Convolution
$B-$ and $\alpha-$spline functions
Filtering theory
FIR digital filters
Principally flat filters

ABSTRACT

$\alpha-$spline functions, which are a generalization of conventional $B-$splines, are defined with several parameters which provide more flexibility in terms of the variety of shapes that the functions can adopt. Because of this feature, the $\alpha-$spline functions have shown improvements in the performance of several applications, including the design of digital filters. This article proposes a novel parametrization to generate new families of $\alpha-$spline functions that allows a more efficient control of the shape of these functions. Different combinations of parameters are presented, and a detailed analysis of the properties of the new functions is carried out. In addition, the new $\alpha-$spline functions are applied to the design of digital filters, providing an appropriate design procedure. The characteristics of the new filters are analysed and compared with previous design techniques, demonstrating the remarkable superiority of their performance.

© 2022 The Authors. Published by Elsevier B.V.
This is an open access article under the CC BY-NC-ND license
(http://creativecommons.org/licenses/by-nc-nd/4.0/)

1. Introduction

Spline functions are a tool widely used in various fields of science and engineering. They are used in graphic design [1–3], in the treatment and reconstruction of diverse signals [4], including images [5,6], in the numerical resolution of differential equations [7], to improve the performance of signal processing tools [8,9], and also in control theory for model inversion, such as the design of feedforward actions based on model stable inversion [10–12]. Over time, the fields of application have been expanding and the way to obtain splines has been adapted to the different requirements of the applications.

One way of constructing different spline bases is by means of repetitive convolution processes of the spline base of degree 0, that is, a non-zero constant function between two consecutive nodes and zero outside this interval. The constant is chosen so that the enclosed area is one, and if the set of nodes are integers, which is a common case, then the constant must be exactly one. From this perspective, several variants of spline bases in the time domain have been proposed, providing new tools that present, in specific applications, certain advantages over the original $B-$spline bases. Examples of this are the spline bases proposed in time-domain in [13,14] that are defined by the convolution of two types of rectangular pulses, one with a fixed width and the other with a width dependent on an adjustable parameter, so that a continuous transition between two basic or natural spline orders can be achieved. They constitute a set of functions whose shape is adjustable by means of one or several parameters that allow a smooth transition between spline functions of integer orders.

In this work, we focus our attention on [14], where a set of transitional functions ($\alpha-$spline) between linear (first-order) $B-$spline functions and cubic (third-order) $B-$spline functions, is introduced. The proposed $\alpha-$splines are used in interpolation processes for the reconstruction of signals. In certain applications, $\alpha-$splines outperform the classic $B-$spline bases, [15,16]. $B-$spline kernels are constructed from the convolution of unit-width rectangular pulses. In contrast, the $\alpha-$spline are the result of convolving rectangular pulses of unit- and $\alpha-$width. As a result, $\alpha-$spline functions result in transition functions between two B$-$spline functions, where the latter are a particular case of the former. Therefore, the range of possible (real) applications where $\alpha-$splines can be applied is too broad, including at least those of B$-$spline functions.

Digital filter design is a classical area of signal processing that still sparks the interest of many researchers [17–21]. The application of spline functions to digital filter design, according to cer-

* Corresponding author.
E-mail address: miguel.raposo@uah.es (M.Á. Raposo–Sánchez).

https://doi.org/10.1016/j.sigpro.2022.108836
0165-1684/© 2022 The Authors. Published by Elsevier B.V. This is an open access article under the CC BY-NC-ND license (http://creativecommons.org/licenses/by-nc-nd/4.0/)

tain optimization criteria, has been proposed in [22–26]. The use of spline bases for designing digital filters allows to generate transition bands that continuously connect the passband and the stopband of the filter, eliminating the discontinuities in the limits of these bands. As a result, the frequency response of the designed filter presents a quadratic error very close to the optimum value, corresponding to the ideal filter. In addition, the use of spline functions provides explicit control over the transition band and an approximation almost as good as the most complicated numerical approximations. The resulting FIR filters are easy to design by means of previously determined closed expressions. In [22,23], $B-$spline functions are employed as window functions to shape the transition band of the conventional brick-wall ideal filter. From the spline base of degree 0, that is, a rectangular function in the frequency domain, the base spline of a degree $l \geq 0$ is constructed by convolving $l+1$ spline bases of degree 0, giving rise to a potential function in the time domain, which takes the form of sinc^{l+1}. The power of the sinc function is called spline order. In [25], the mathematical framework to extend the above design methods to positive non-integer order is presented. In [26], $\alpha-$spline analog filters, and the design of digital filters by a least integral squared error approximation and principally flat $\alpha-$spline filters are discussed.

This article has a twofold purpose. First, four novel families of $\alpha-$spline functions, defined by means of two parameters k_1 and k_2, are introduced.The new formulation allows more precise control to set the shape of the function. The formulation is derived in the frequency domain associated with discrete time, since the second objective of the article is to present as a case study the application of these new families to digital filter design. However, it is worth noting that the resulting expressions can be interchanged between domains using the duality property of the Fourier transform[1]. To the aim of completing the theory presented in our previous works [25,26], we use here the new $\alpha-$spline functions to design digital filters. The obtained filters are compared to those previously reported in the literature [22,23,25,26]. Specifically, the characteristics of the new filters are analyzed and compared with previous $\alpha-$ and B$-$spline-based approaches. The simulation results indicate that with the new $\alpha-$spline functions, it is possible to obtain filters that outperform those designed with previous techniques.

The rest of this paper is organized as follows. In Section 2, the formulation of the $\alpha-$spline functions is presented. In Section 3, closed expressions of the $\alpha-$spline functions are derived. Next, Section 4 analyses the sizes of the compact supports of the different families of $\alpha-$spline functions. Section 5 presents the process of designing digital filters and their main features. Afterwards, some design examples are presented and, lastly, the conclusions of this paper are presented.

2. A new definition of the generalized α-spline functions

This section presents an extension of the α-spline functions previously described in [25]. The new functions, defined in the frequency domain, are generated by the convolution of two kinds rectangular pulses of area 2π (degree 0 spline bases) and form a set of transition functions between spline bases of degrees p and $p+q$. These functions gradually transform a spline base of degree $p \geq 0$ into a spline base of degree $p+q$, $q>0$. The variation of the width and height of both pulses will determine the shape and compact support of the new α-spline bases. These two types of rectangular pulses are defined by

$$\Phi^{[0]}_{k_1,\Delta_d}(\omega) = \begin{cases} \frac{2\pi k_1}{\Delta_d}, & |\omega| < \frac{\Delta_d}{2k_1}, \\ 0, & \frac{\Delta_d}{2k_1} < |\omega| < \pi, \end{cases} \tag{1}$$

and

$$\Phi^{[0]}_{k_2,\alpha\Delta_d}(\omega) = \begin{cases} \frac{2\pi k_2}{\alpha\Delta_d}, & |\omega| < \frac{\alpha\Delta_d}{2k_2}, \\ 0, & \frac{\alpha\Delta_d}{2k_2} < |\omega| < \pi, \end{cases} \tag{2}$$

where ω is the frequency with dimensions of radians per sample, Δ_d is a parameter with the same units, which governs the support of the α-spline function in the frequency domain, k_1 and k_2 are two constants from which we will define different families of spline bases. Finally, $\alpha \in (0,1)$, is dimensionless and controls the transition between two spline bases.

By convolution of $p+1$ rectangular pulses, given by (1), the spline basis function of constant k_1 and p degree, $\left(\Phi^{[p]}_{k_1,\Delta_d}(\omega)\right)$, is constructed, that is,

$$\Phi^{[p]}_{k_1,\Delta_d}(\omega) = \overbrace{\Phi^{[0]}_{k_1,\Delta_d}(\omega) * \ldots * \Phi^{[0]}_{k_1,\Delta_d}(\omega)}^{(p+1)\text{ spline base } \Phi^{[0]}_{k_1,\Delta_d}}. \tag{3}$$

Similarly, the convolution of q rectangular pulses given by (2), generates the spline basis function of constant k_2 and $(q-1)$ degree, $\left(\Phi^{[q-1]}_{k_2,\alpha\Delta_d}(\omega)\right)$, that is,

$$\Phi^{[q-1]}_{k_2,\alpha\Delta_d}(\omega) = \overbrace{\Phi^{[0]}_{k_2,\alpha\Delta_d}(\omega) * \ldots * \Phi^{[0]}_{k_2,\alpha\Delta_d}(\omega)}^{q\text{ spline base } \Phi^{[0]}_{k_2,\alpha\Delta_d}}. \tag{4}$$

By the convolution of (3) and (4) the transition functions (new α-spline base functions) are constructed. Let $\Phi^{[p,p+q,\alpha]}_{k_1,k_2,\Delta_d}(\omega)$ denote the new α-spline base function, then

$$\Phi^{[p,p+q,\alpha]}_{k_1,k_2,\Delta_d}(\omega) = \Phi^{[p]}_{k_1,\Delta_d}(\omega) * \Phi^{[q-1]}_{k_2,\alpha\Delta_d}(\omega),$$

$$\Psi^{[p,p+q,\alpha]}_{k_1,k_2,\Delta_d}(\omega) = \overbrace{\Phi^{[0]}_{k_1,\Delta_d}(\omega) * \ldots * \Phi^{[0]}_{k_1,\Delta_d}(\omega)}^{(p+1)\text{ spline base } \Phi^{[0]}_{k_1,\Delta_d}}$$
$$* \overbrace{\Phi^{[0]}_{k_2,\alpha\Delta_d}(\omega) * \ldots * \Phi^{[0]}_{k_2,\alpha\Delta_d}(\omega)}^{q\text{ spline base } \Phi^{[0]}_{k_2,\alpha\Delta_d}}. \tag{5}$$

Hereinafter, the frequency range considered for the Fourier transforms will be $-\pi < \omega \leq \pi$. We proceed first by calculating the inverse DTFT of (1):

$$f_{k_1,\Delta_d}[n] = \mathfrak{F}^{-1}\left\{\Phi^{[0]}_{k_1,\Delta_d}(\omega)\right\} = \text{sinc}\left(\frac{\Delta_d n}{2\pi k_1}\right) = \frac{k_1}{\Delta_d(-jn)}\left[e^{-j\frac{\Delta_d n}{2k_1}} - e^{j\frac{\Delta_d n}{2k_1}}\right], \tag{6}$$

where the function sinc is defined as $\text{sinc}(x) = \sin(\pi x)/(\pi x)$. Similarly, the inverse DTFT of (2) is given by

$$f_{k_2,\alpha\Delta_d}[n] = \mathfrak{F}^{-1}\left\{\Phi^{[0]}_{k_2,\alpha\Delta_d}(\omega)\right\} = \text{sinc}\left(\frac{\alpha\Delta_d n}{2\pi k_2}\right) = \frac{k_2}{\alpha\Delta_d(-jn)}\left[e^{-j\frac{\alpha\Delta_d n}{2k_2}} - e^{j\frac{\alpha\Delta_d n}{2k_2}}\right]. \tag{7}$$

From (6) and (7) and considering the properties of the convolution operation, we get the inverse DTFT of $\Phi^{[p,p+q,\alpha]}_{k_1,k_2,\Delta_d}(\omega)$

$$F^{[p,p+q,\alpha]}_{k_1,k_2,\Delta_d}[n] = \mathfrak{F}^{-1}\left\{\Phi^{[p,p+q,\alpha]}_{k_1,k_2,\Delta_d}(\omega)\right\} = \text{sinc}^{p+1}\left(\frac{\Delta_d n}{2\pi k_1}\right)\cdot\text{sinc}^{q}\left(\frac{\alpha\Delta_d n}{2\pi k_2}\right), \tag{8}$$

or, in terms of the complex exponential functions,

$$F^{[p,p+q,\alpha]}_{k_1,k_2,\Delta_d}[n] = \frac{k_1^{p+1}k_2^{q}}{\alpha^{q}\Delta_d^{p+1+q}(-jn)^{p+1+q}}\frac{\left(e^{-j\frac{\Delta_d n}{2k_1}} - e^{j\frac{\Delta_d n}{2k_1}}\right)^{p+1}}{\left(e^{-j\frac{\alpha\Delta_d n}{2k_2}} - e^{j\frac{\alpha\Delta_d n}{2k_2}}\right)^{-q}}. \tag{9}$$

[1] For the time-domain formulation, we refer the reader to [27]

We can rewrite the above function by developing the powers of the binomials:

$$F_{k_1,k_2,\Delta_d}^{[p,p+q,\alpha]}[n] = \frac{k_1^{p+1}k_2^q}{\alpha^q \Delta_d^{p+1+q}(-jn)^{(p+1+q)}} \cdot \sum_{k=0}^{p+1}\sum_{l=0}^{q} C_{kl} e^{j\Gamma_{k_1,k_2}^{[p,q,\alpha]}(k,l)\Delta_d n}, \tag{10}$$

where C_{kl} and $\Gamma_{k_1,k_2}^{[p,q,\alpha]}(k,l)$ are given respectively by

$$C_{kl} = (-1)^{(k+l)}\begin{pmatrix} p+1 \\ k \end{pmatrix}\begin{pmatrix} q \\ l \end{pmatrix}, \tag{11}$$

and

$$\Gamma_{k_1,k_2}^{[p,q,\alpha]}(k,l) = \left[\left(\frac{k}{k_1}+\frac{\alpha l}{k_2}\right) - \frac{1}{2}\left(\frac{p+1}{k_1}+\frac{\alpha q}{k_2}\right)\right], \tag{12}$$

which, for later use, is expressed as

$$\Gamma_{k_1,k_2}^{[p,q,\alpha]}(k,l) = \Gamma_1(k,l) - \Gamma_2,$$

with

$$\Gamma_1(k,l) = \left(\frac{k}{k_1}+\frac{\alpha l}{k_2}\right) \quad \text{and} \quad \Gamma_2 = \frac{1}{2}\left(\frac{p+1}{k_1}+\frac{\alpha q}{k_2}\right). \tag{13}$$

From the discrete time domain representation of the new transition functions (8), we associate to them an intermediate spline order (non-integer order) between the starting spline order (power of the first sinc function, $p+1$) and the maximum spline order (sum of the powers of the sinc functions when $\alpha = 1$, $p+1+q$), proportional to α and given by the real number $\rho = p+1+\alpha q$.

3. Polynomial form in the frequency domain

The aim of this section is to express the α-spline functions in polynomial form, since in this way it is relatively straightforward to obtain and analyse closed expressions without resorting to numerical approximations. In addition, this polynomial form makes it possible to impose conditions on their continuity and derivability that are useful in certain applications (e.g. filtering). First, the DTFT of (10) will be determined. With this goal, the auxiliary function $Y_{+,\ell}(\omega)$ is considered, which is defined by

$$Y_{+,\ell}(\omega) = \omega_+^\ell = \begin{cases} \omega^\ell, & 0 \le \omega < \pi, \\ 0, & -\pi \le \omega < 0, \end{cases} = \omega^\ell \cdot u(\omega), \ -\pi \le \omega < \pi$$

where $\ell \in \mathbb{N}$ and $u(\omega)$ is the Heaviside step function. Differentiating repeatedly yields

$$\frac{d^{(\ell)}Y_{+,\ell}(\omega)}{d\omega^\ell} = \ell! \cdot u(\omega) = \mathfrak{F}\left\{(-jn)^\ell y_\ell[n]\right\}, \quad -\pi \le \omega < \pi$$

$$\frac{d^{(\ell+1)}Y_{+,\ell}(\omega)}{d\omega^{\ell+1}} = \ell! \cdot \delta(\omega) = \mathfrak{F}\left\{(-jn)^{\ell+1} y_\ell[n]\right\}, \quad -\pi \le \omega < \pi$$

where $\delta(\omega)$ is the Dirac Delta function and $y_\ell[n]$ is the inverse DTFT of $Y_{+,\ell}(\omega)$.

Calculating the inverse DTFT in the last expression yields

$$\mathfrak{F}^{-1}\{\ell!\delta(\omega)\} = \mathfrak{F}^{-1}\left\{\mathfrak{F}\left\{(-jn)^{\ell+1}y_\ell[n]\right\}\right\}, \quad -\pi \le \omega < \pi$$

and as $\mathfrak{F}^{-1}\{\delta(\omega)\} = 1/(2\pi)$ in $-\pi \le \omega < \pi$, one can write

$$\frac{\ell!}{2\pi} = (-jn)^{\ell+1}y_\ell[n],$$

and therefore

$$y_\ell[n] = \frac{\ell!}{2\pi(-jn)^{\ell+1}}. \tag{14}$$

By replacing $\ell = p+q$, we get

$$\frac{1}{(-jn)^{p+1+q}} = \frac{2\pi y_{p+q}[n]}{(p+q)!}. \tag{15}$$

The factor $(-jn)^{p+1+q}$ appears in the time sequence $F_{k_1,k_2,\Delta_d}^{[p,p+q,\alpha]}[n]$. Substituting (15) in (10) yields

$$F_{k_1,k_2,\Delta_d}^{[p,p+q,\alpha]}[n] = \frac{2\pi k_1^{p+1}k_2^q}{\alpha^q \Delta_d^{p+1+q}(p+q)!} \cdot \sum_{k=0}^{p+1}\sum_{l=0}^{q} C_{kl} e^{j\Gamma_{k_1,k_2}^{[p,q,\alpha]}(k,l)\Delta_d n} y_{p+q}[n]. \tag{16}$$

Calculating the DTFT of (16) and using the properties of linearity and displacement in frequency, the functions α-spline, $\Phi_{k_1,k_2,\Delta_d}^{[p,p+q,\alpha]}(\omega) = \mathfrak{F}\left\{F_{k_1,k_2,\Delta_d}^{[p,p+q],\alpha}[n]\right\}$, can be expressed in polynomial form as

$$\Phi_{k_1,k_2,\Delta_d}^{[p,p+q,\alpha]}(\omega) = \frac{2\pi k_1^{p+1}k_2^q}{\alpha^q \Delta_d^{p+1+q}(p+q)!} \cdot \sum_{k=0}^{p+1}\sum_{l=0}^{q} C_{kl} Y_{+,\,p+q}[\omega - \Gamma_{k_1,k_2}^{[p,q,\alpha]}(k,l)\Delta_d] \tag{17}$$

$$= \frac{2\pi k_1^{p+1}k_2^q}{\alpha^q \Delta_d(p+q)!} \cdot \sum_{k=0}^{p+1}\sum_{l=0}^{q} C_{kl}\left\{\frac{\omega}{\Delta_d} - \Gamma_{k_1,k_2}^{[p,q,\alpha]}(k,l)\right\}_+^{p+q}, \tag{17}$$

which are valid for any value $-\pi \le \omega < \pi$. These functions $\Phi_{k_1,k_2,\Delta_d}^{[p,p+q,\alpha]}(\omega)$ are periodic, of period 2π, and have a finite compact support. This means they are different from zero in a spectral interval given by

$$-\Gamma_2\,\Delta_d < \omega < \Gamma_2\,\Delta_d, \tag{18}$$

which depends on the number of pulses involved in the convolution.

Fig. 1 shows a set of α-spline functions that perform a continuous transition between a spline base of class $k_1 = 2$ and degree $p = 1$ to another spline base of class $k_2 = 1.5$ and degree $p+q = 2$, for $\Delta_d = 0.1\pi$ as the parameter value. In this figure, notice that the curves for $\alpha = 0$ and $\alpha = 1$ correspond to B-spline bases of degree 1 and 2, respectively.

4. Properties of the α-spline functions

Different values of k_1 and k_2 in the definition of the initial rectangular pulses (1) and (2) determine several families of bases α-spline. To illustrate the properties of the new α-spline function, from the wide range of possible combinations of parameters k_1 and k_2, four possibilities have been selected, which are reflected in Table 1.

The functions of the first family, characterized by $k_1 = k_2 = p+1+\alpha q$, have a compact support that only depends on Δ_d, being independent from the rest of the parameters that are involved in its definition. This support, according to (13) and (18), is given by

$$-\frac{\Delta_d}{2} < \omega < \frac{\Delta_d}{2}.$$

In Fig. 2 are represented some α-spline functions belonging to the first family. All of them, regardless of their order or the value of the parameter α, have the same compact support size, that matches the value assigned to $\Delta_d = 0.2\pi$.

The functions of the second family, characterized by $k_1 = p+1$ and $k_2 = q$, have a compact support that depends on the parameter α, in addition to Δ_d, and increases with them and, according to (13) and (18), is given by

$$-(1+\alpha)\frac{\Delta_d}{2} < \omega < (1+\alpha)\frac{\Delta_d}{2}.$$

Fig. 3 depicts some α-spline functions belonging to the second family. It can be seen that setting the value of $\Delta_d = 0.25\pi$, the

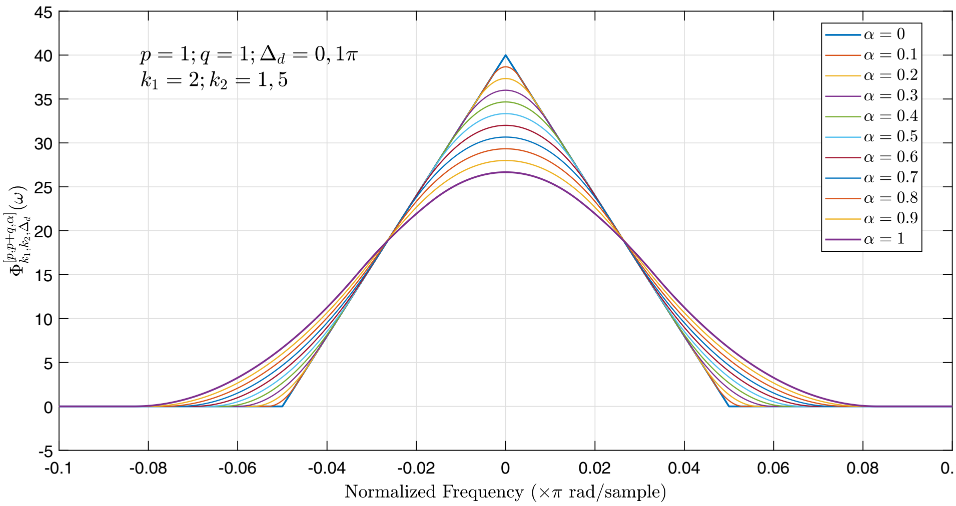

Fig. 1. Transitional α-spline bases $\left(\Phi^{[1,2,\alpha]}_{2,1.5,0.1\pi}(\omega)\right)$ for different values of α. B-spline bases of degree 1 and 2 correspond to $\alpha = 0$ and $\alpha = 1$, respectively..

Table 1
Different families of α-spline functions defined on the frequency domain.

Parameters	α-spline base Family 1	α-spline base Family 2	α-spline base Family 3	α-spline base Family 4
k_1	$p+1+\alpha q$	$p+1$	1	q
k_2	$p+1+\alpha q$	q	αq	$p+1$

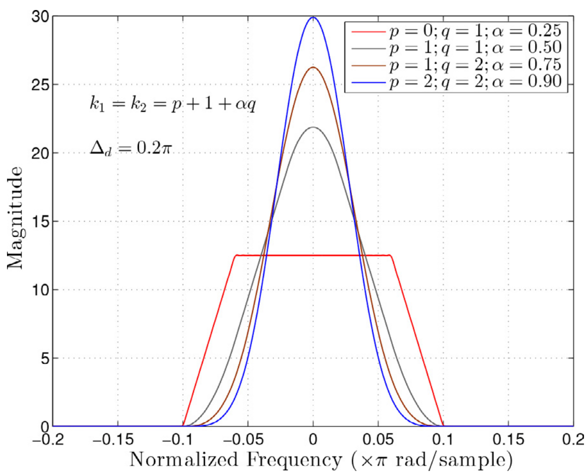

Fig. 2. α-spline bases $\left(\Phi^{[p,p+q,\alpha]}_{(p+1+\alpha q),(p+1+\alpha q),\Delta_d}(\omega)\right)$ of Family 1.

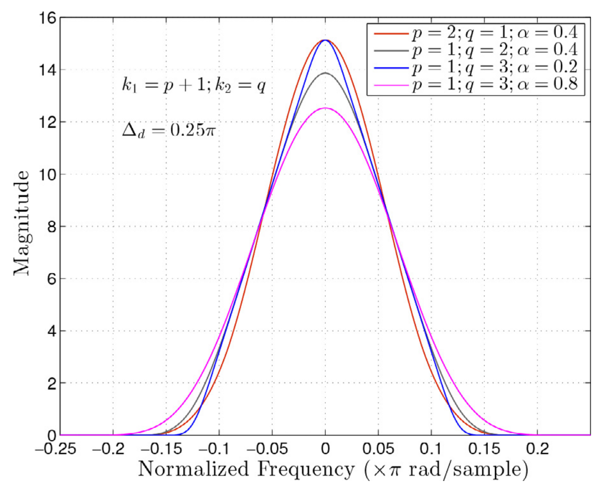

Fig. 3. α-spline bases $\left(\Phi^{[p,p+q,\alpha]}_{(p+1),q,\Delta_d}(\omega)\right)$ of Family 2.

compact support of all the functions only depends on α, increasing with this parameter, and being independent of the numbers of pulses, $(p+1)$ and q, that shape the α-spline base.

The functions of the third family, characterized by $k_1 = 1$ and $k_2 = \alpha q$, have a compact support that depends on the number of pulses $p+1$ defined by (1), in addition to Δ_d, being increasing with both parameters. According to (13) and (18), the compact support is given by

$$-(p+2)\frac{\Delta_d}{2} < \omega < (p+2)\frac{\Delta_d}{2}.$$

Fig. 4 shows some α-spline bases belonging to this family. It can be observed that, for a fixed value of $\Delta_d = 0.2\pi$, the compact support only depends on the value of p, being increasing with this parameter.

The functions of the fourth family, characterized by $k_1 = q$ and $k_2 = p+1$, have a compact support that depends on all the parameters Δ_d, α, p and q. According to (13) and (18), the compact support is given by

$$-\left(\frac{p+1}{q} + \frac{\alpha q}{p+1}\right)\frac{\Delta_d}{2} < \omega < \left(\frac{p+1}{q} + \frac{\alpha q}{p+1}\right)\frac{\Delta_d}{2}.$$

Fig. 5 plots some α-spline bases belonging to this family. It shows how, for a fixed value of $\Delta_d = 0.25\pi$, the compact support changes, depending both on the parameter α and the number of pulses of the two types used to generate the different α-spline functions.

Lastly, with the aim of showing the different profiles obtained with k_1 and k_2, Fig. 6 depicts normalized functions defined as

$$\frac{\Phi^{[p,p+q,\alpha]}_{k_1,k_2,\Delta_d}(\omega)}{\Phi^{[p,p+q,\alpha]}_{k_1,k_2,\Delta_d}(0)}$$

for both the same α-spline order $\{(p+1), q, \alpha\}$ and compact support $\Delta_{ef} = 0.2\,\pi$. These functions belong to each one of the families defined in Table 1.

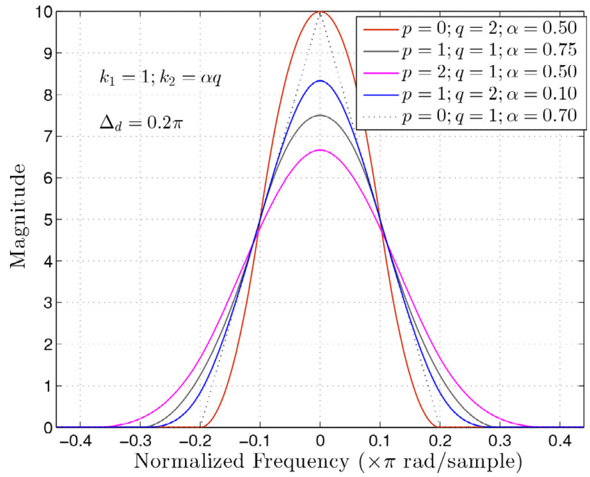

Fig. 4. α-spline bases $\left(\Phi^{[p,p+q,\alpha]}_{1,\alpha q,\Delta_d}(\omega)\right)$ of Family 3.

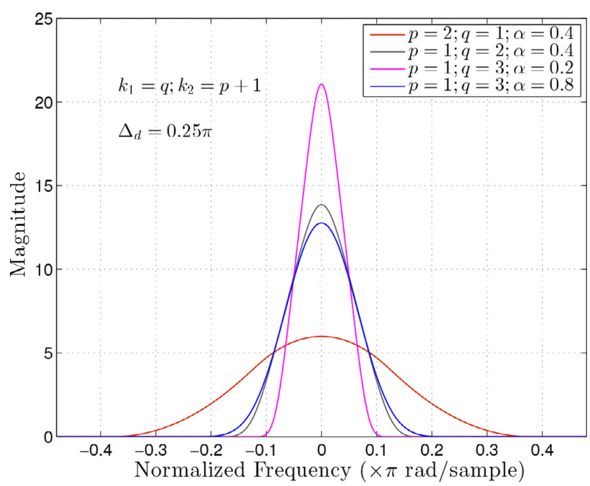

Fig. 5. α-spline bases $\left(\Phi^{[p,p+q,\alpha]}_{q,p+1,\Delta_d}(\omega)\right)$ of Family 4.

5. Application to digital filter design

5.1. Modeling of transition bands with α-spline bases

Consider a digital filter with impulse response $h_\alpha[n]$ and frequency response

$$H_\alpha(\omega)=\sum_{n=-\infty}^{\infty} h_\alpha[n]e^{-j\omega n}.$$

Let us consider an ideal low-pass filter, with a cut-off frequency of ω_c and whose frequency response is represented by $H_d(\omega)$. The proposed design procedure is based on the convolution in the frequency domain between the frequency response of the ideal brick-wall filter and an α−spline function (window) of the set given by (17), $\Phi^{[p,p+q,\alpha]}_{k_1,k_2,\Delta_d}(\omega)$, that is,

$$\begin{aligned}H_\alpha(\omega)&=\Phi^{[p,p+q,\alpha]}_{k_1,k_2,\Delta_d}(\omega)*H_d(\omega)\\&=\frac{1}{2\pi}\int_{-\pi}^{\pi}\Phi^{[p,p+q,\alpha]}_{k_1,k_2,\Delta_d}(\xi)H_d(\omega-\xi)d\xi.\end{aligned}\tag{19}$$

As can be seen in [25], (19) is composed of polynomial functions, and the resulting frequency response is given by

$$H_\alpha(\omega)=1-\frac{k_1^{p+1}k_2^q}{\alpha^q(p+q+1)!}\cdot\sum_{k=0}^{p+1}\sum_{l=0}^{q}C_{kl}\left\{\frac{|\omega|-\omega_c}{\Delta_d}-\Gamma^{[p,q,\alpha]}_{k_1,k_2}(k,l)\right\}_+^{p+q+1},\tag{20}$$

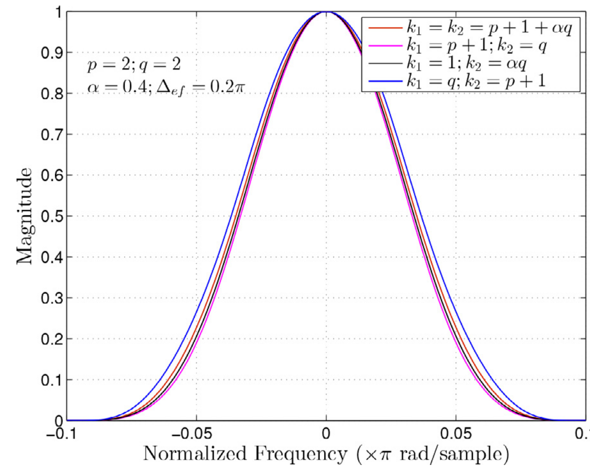

Fig. 6. Spline families. Normalized α-spline bases of the same order $\left(\Phi^{[p,p+q,\alpha]}_{k_1,k_2,\Delta_d}(\omega)\right)$.

where $-\pi\le\omega<\pi$, $0<\alpha<1$, $p\ge 0$ and $q>0$. The shape of the frequency response of the filter (20) is determined by the symmetry properties and compact support of the $\Phi^{[p,p+q,\alpha]}_{k_1,k_2,\Delta_d}(\omega)$, but in general, it takes the following forms:

$$H_\alpha(\omega)=\begin{cases}1, & 0<|\omega|<(\omega_c-\Gamma_2\,\Delta_d),\\ \in(0,1), & (\omega_c-\Gamma_2\Delta_d)<|\omega|<(\omega_c+\Gamma_2\,\Delta_d),\\ 0, & (\omega_c+\Gamma_2\Delta_d)<|\omega|<\pi,\end{cases}\tag{21}$$

where the shape and width of the transition band depends on the α-spline function used.

5.1.1. Continuity and differentiability

This section highlights some of the general properties of the α-spline functions such as their smoothness and their ability to approximate a step function with different shapes and velocities. This will provide us with some information about the transition band of the resulting filters. To begin with, it is important to note that the results are independent of the parameters that define the filter, thus a variable change is proposed to normalize the width of the transition band so as to lie within the [0,1] interval. In addition, instead of using the frequency response of the low-pass filter given by (20), the analysis of the properties is carried out on the associated high-pass function $G_\alpha(\omega)=1-H_\alpha(\omega)$. Because the function is symmetrical with respect to the frequency, we will focus on the positive interval of the frequency, i.e. $0\le\omega\le\pi$. In terms of $\Gamma_1(k,l)$ and Γ_2, Eq. (20) is expressed as

$$G_\alpha(\omega)=\frac{k_1^{p+1}k_2^q}{\alpha^q(p+q+1)!}\cdot\sum_{k=0}^{p+1}\sum_{l=0}^{q}C_{kl}\left\{\frac{\omega-\omega_c}{\Delta_d}-\Gamma_1(k,l)+\Gamma_2\right\}_+^{p+q+1},\tag{22}$$

whose transition band occupies the interval $\omega_c-\Gamma_2\Delta_d\le\omega\le\omega_c+\Gamma_2\Delta_d$.

We can rewrite the above expression in the form

$$\begin{aligned}G_\alpha(\omega)=&\frac{k_1^{p+1}k_2^q}{\alpha^q(p+q+1)!}\\&\cdot\sum_{k=0}^{p+1}\sum_{l=0}^{q}C_{kl}\left\{\Gamma_2\left(\frac{\omega-\omega_c}{\Gamma_2\Delta_d}+1\right)-\Gamma_1(k,l)\right\}_+^{p+q+1}.\end{aligned}\tag{23}$$

By making the change of variable

$$\frac{\omega-\omega_c}{\Gamma_2\Delta_d}+1=2x,$$

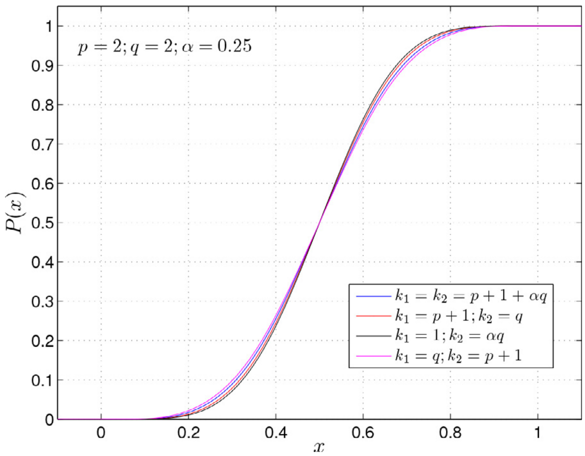

Fig. 7. High-Pass Filters ($P(x)$).

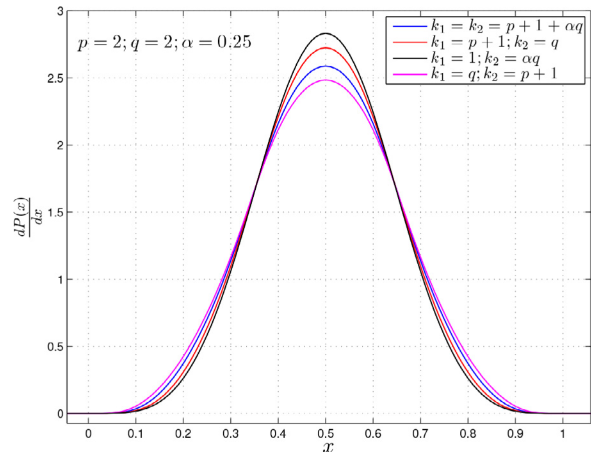

Fig. 8. First derivative of high-pass filters ($\frac{dP(x)}{dx}$).

we obtain a function that depends on the variable x, which we will call $P(x)$, and that acquires the form

$$P(x) = \frac{k_1^{p+1} k_2^q}{\alpha^q (p+q+1)!} \sum_{k=0}^{p+1} \sum_{l=0}^{q} C_{kl} \{2\Gamma_2 x - \Gamma_1(k,l)\}_+^{p+q+1}, \tag{24}$$

where both the ends of the transition band and the cutoff frequency are determined by the value of the variable x:

$$x = \begin{cases} 0, & \omega = \omega_c - \Gamma_2 \Delta_d, \\ \frac{1}{2}, & \omega = \omega_c, \\ 1, & \omega = \omega_c + \Gamma_2 \Delta_d. \end{cases}$$

It can be shown that $P(x)$ is continuous on [0,1] and positive definite on (0,1); furthermore, it satisfies

$$P(x) = \begin{cases} 0, & x \le 0, \\ \in (0,1), & x \in (0,1), \\ 1, & x \ge 1. \end{cases}$$

As a result, $P(x)$ can be interpreted as a smoothed step function that is continuous and differentiable. Taking into account its polynomial form, its derivative is

$$P'(x) = \frac{k_1^{(p+1)} k_2^q}{(p+q)!\alpha^q} (2\Gamma_2)^{(p+1+q)} \sum_{k=0}^{p+1} \sum_{l=0}^{q} C_{kl} \{x - N_{kl}\}_+^{p+q}, \tag{25}$$

where

$$N_{kl} = \frac{\Gamma_1(k,l)}{2\Gamma_2} = \left(\frac{k_2 k + k_1 \alpha l}{k_2(p+1) + k_1 \alpha q} \right).$$

This derived function maintains the functional structure of $P(x)$ and is another continuous function on [0,1] and positive definite on (0,1). Therefore, $P(x)$ is a positive and strictly increasing function in that interval. Iteratively, it can be shown that $P(x)$ has $(p+q)$ derivatives in (0,1). Fig. 7 shows the functions given by (24) for all the previously defined families and considering the same order, $p = 2$, $q = 2$ and $\alpha = 0.25$. As can be seen, both the range and the domain of the functions are located in the [0,1] interval, being continuous, differentiable, and monotone-increasing. In Fig. 8, which depicts the derivatives of the previous functions, different growth rates in the high-pass functions can be observed.

5.2. Impulse response of the digital filter

Given the impulse response of the ideal brick-wall filter

$$h_d[n] = \frac{\omega_c}{\pi} \text{sinc}\left(\frac{\omega_c n}{\pi}\right), \tag{26}$$

the impulse response of the α-spline filter is

$$\begin{aligned} h_\alpha[n] &= h_d[n] \cdot F_{k_1,k_2,\Delta_d}^{[p,p+q,\alpha]}[n] \\ &= \frac{\omega_c}{\pi} \text{sinc}\left(\frac{\omega_c n}{\pi}\right) \text{sinc}^{p+1}\left(\frac{\Delta_d n}{2\pi k_1}\right) \text{sinc}^q\left(\frac{\alpha \Delta_d n}{2\pi k_2}\right). \end{aligned} \tag{27}$$

The interpretation in the frequency domain is that the α-spline functions are used to model the transition band of (21), defined between the pass-band and the stop-band. In the time domain, it turns out that $h_\alpha[n]$ can be written as $h_\alpha[n] = h_d[n] \cdot w[n]$, where the α-spline represent the window function $w[n]$:

$$w[n] = \text{sinc}^{p+1}\left(\frac{\Delta_d n}{2\pi k_1}\right) \text{sinc}^q\left(\frac{\alpha \Delta_d n}{2\pi k_2}\right). \tag{28}$$

It is important to note that the impulse responses, given by (27), are infinite in length and generate non-causal filters. In addition, they are symmetrical around $n = 0$, since they are obtained as the product of two symmetrical functions.

5.3. FIR filters derived from α-spline functions

Finite impulse response filters can be obtained by truncating the impulse response. The resulting $N = 2M + 1$ coefficients are given by

$$h[n] = \begin{cases} h_\alpha[n], & |n| \le M, \\ 0, & |n| > M. \end{cases}$$

For simplicity, real valued and symmetric $h_\alpha[n] = h_\alpha[-n]$ digital filters with length $(2M + 1)$ will be discussed in this paper.

However, this operation generates a problem, because depending on where the truncation occurs and the order of the spline functions used, the spectral behavior changes noticeably. These problems have been analysed in [22,23,25] and [26], using different spline functions and providing different solutions depending on the pursued objective.

Once the FIR filter is obtained, a causal response can be constructed by introducing an M-sample delay, so that the impulse response becomes $h_c[n] = h_\alpha[n - M]$, with $0 \le n \le 2M$. In these conditions, the resulting filter has linear phase.

5.4. Examples: design and discussion

In this subsection, several digital filters are designed with the goal of highlighting the properties of the new α-spline functions. For the sake of comparison, we focus our attention on some of the examples presented in previous publications [23,25,26]. In the above, the design of principally flat filters is considered and the resulting filters are compared either with *B*-spline or with α-spline functions belonging to the family 1 (see Table 1).

The compact support of the α-spline functions depends on both Δ_d and k_1 and k_2. Therefore, in order to obtain a given transition bandwidth, denoted by Δ_r, the width of the compact support of the α-spline functions must be normalized, making $2\Gamma_2\Delta_d = \Delta_r$. According to this, (27) turns out to be

$$h'_\alpha[n] = \frac{\omega_c}{\pi}\mathrm{sinc}\left(\frac{\omega_c n}{\pi}\right)\mathrm{sinc}^{p+1}\left(\frac{\Delta_r n}{2\pi\Gamma k_1}\right)\mathrm{sinc}^{q}\left(\frac{\alpha\Delta_r n}{2\pi\Gamma k_2}\right), \quad (29)$$

where $\Gamma = 2\Gamma_2$. From the considerations outlined in [23] and [25], samples are taken within the interval between the first zero crossings, located to the right and left of the spline origin. Due to the reasons brought out in those publications about the decrease of the average quadratic error, and particularizing for the case of the α-spline functions described there, in which $k_1 = k_2 = p + 1 + \alpha q$ and $\Gamma = 1$, one obtains

$$\frac{\Delta_r}{2\pi(p+1+\alpha q)} = \frac{1}{M+1}. \quad (30)$$

As a result, the impulse response is given by

$$h^{(1)}_{PF,\alpha}[n] = \frac{\omega_c}{\pi}\mathrm{sinc}\left(\frac{\omega_c n}{\pi}\right)\mathrm{sinc}^{p+1}\left(\frac{n}{M+1}\right) \times \mathrm{sinc}^{q}\left(\frac{\alpha n}{M+1}\right), \ -M \le n \le M, \quad (31)$$

where the superscript (1) stands for the family 1 (Table 1).

In our example of designs, the different behaviors in the frequency response will be shown using α-spline functions of the same order, but characterized by different values of k_1 and k_2. From (29), for any combination of k_1 and k_2 and with the constraint imposed by (30), the impulse response turns out to be

$$h'_{PF,\alpha}[n] = \frac{\omega_c}{\pi}\mathrm{sinc}\left(\frac{\omega_c n}{\pi}\right)\mathrm{sinc}^{p+1}\left(\frac{(p+1+\alpha q)n}{\Gamma k_1(M+1)}\right) \times \mathrm{sinc}^{q}\left(\frac{\alpha(p+1+\alpha q)n}{\Gamma k_2(M+1)}\right), \ -M \le n \le M. \quad (32)$$

To compare the characteristics of the designed filters, we employ the following quality parameters:

- The average integral squared approximation error, ε_{aisae}, defined as

$$\varepsilon_{aisae} = \sum_{n=-M}^{M}\left|h_d[n] - h'_{PF,\alpha}[n]\right|^2 + 2\sum_{n=M}^{\infty}|h_d[n]|^2.$$

- The passband error, ε_{pbe}, given by

$$\varepsilon_{pbe} = \frac{1}{\pi}\int_0^{\omega_p}\left|H'_{PF,\alpha}(\omega) - H_d(\omega)\right|^2 d\omega,$$

  where $H'_{PF,\alpha}(\omega)$ is the frequency response associated with the impulse response given by (32).
- The stopband error, ε_{sbe}, given by

$$\varepsilon_{sbe} = \frac{1}{\pi}\int_{\omega_s}^{\pi}\left|H'_{PF,\alpha}(\omega)\right|^2 d\omega.$$

- The maximum passband deviation, ε_{dev}, given by

$$\delta = \max_{|\omega|<\omega_p}\left|H'_{PF,\alpha}(\omega) - H_d(\omega)\right|.$$

- The minimum stopband attenuation, A_s (dB).

The first example is the filter proposed in Section 4 of [26], whose desired specifications are

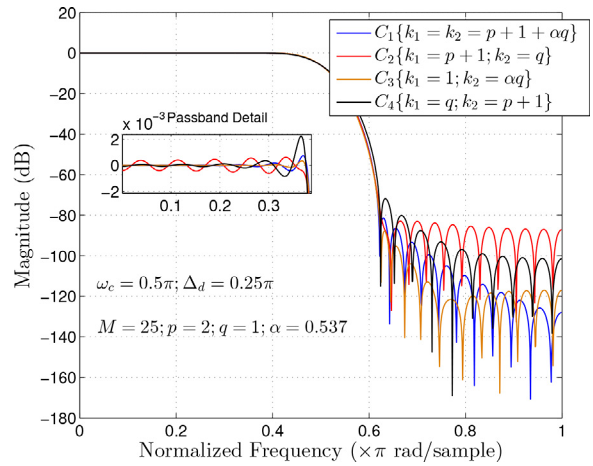

Fig. 9. Example design 1. Magnitude responses for PF low-pass $\alpha-$spline filters.

- Minimum stopband attenuation $A_s = 80$ dB,
- Cutoff frequency $\omega_c = 0.5\pi$,
- Transition bandwidth $\Delta_r = 0.25\pi$,

Considering the procedures to obtain M and $\rho = p + 1 + \alpha q$, described in [23, Table 1] or [25, Tables 1 and 2], we obtain the values $M = 25$ and $\rho = p + 1 + \alpha q = 3.537$.

To compare the performance of the resulting filters, we generate α-spline functions of the same order $\{(p+1) = 3,\ q = 1,\ \alpha = 0.537\}$ belonging to the different families of Table 1. They are characterized by different combinations of k_1 and k_2.

The first combination of parameters, $C_1 = \{k_1 = p + 1 + \alpha q,\ k_2 = p + 1 + \alpha q\}$, is the one used in Section 4 of [26]. Next, three new filters are designed with the following parameter combinations: $C_2 = \{k_1 = p + 1,\ k_2 = q\}$, $C_3 = \{k_1 = 1,\ k_2 = \alpha q\}$ and $C_4 = \{k_1 = q,\ k_2 = p + 1\}$.

Fig. 9 depicts the magnitude response of the resulting filters, and Table 2 shows the values of the quality parameters measured in each of them, as well as the effective transition bandwidth, $\Delta_r(\times\pi)$. This table also includes the filter designed with non-integer order *B*-spline functions obtained in [26]. As can be seen, the filter designed with the α-spline function of the C_3 family has significantly higher performance than the rest of the filters.

The second example design is given by the specifications of the low-pass filter described in Section 5 of [25]:

- Minimum stopband attenuation $A_s = 60$ dB,
- Cutoff frequency $\omega_c = 0.25\pi$,
- Transition bandwidth $\Delta_r = 0.05\pi$,

In this example, taken into account [23, Table 1] or [25, Tables 1 and 2], the semi-order of the filter is $M = 90$ and the spline order is $\rho = p + 1 + \alpha q = 2.339$.

In [25], the frequency response of an α-spline filter with values $p + 1 = 1$, $q = 2$ and $\alpha = 0.6695$ ($\rho = p + 1 + \alpha q = 2.339$), belonging to the family $C_1^* = \{k_1 = p + 1 + \alpha q, k_2 = p + 1 + \alpha q\}$ was determined. Now, we proceed to design digital filters with impulse responses given by (32) and satisfying $C_2^* = \{k_1 = p + 1, k_2 = q\}$, $C_3^* = \{k_1 = 1, k_2 = \alpha q\}$ and $C_4^* = \{k_1 = q, k_2 = p + 1\}$.

Fig. 10 plots the resulting magnitude responses, and Table 3 shows the obtained results of the quality parameters of these new filters. As can be seen, in addition to the filter designed from the α-spline function of the C_1^* family, the one generated from the C_4^* family has a higher performance than those achieved by the filters designed using either the *B*-spline function and the rest of the α-spline functions.

Table 2
Simulation results for different low-pass PF filters ($A_s = 80$ dB, $\omega_c = 0.5\pi$, $\Delta_r = 0.25\pi$).

Function	ε_{aisae}	ε_{pbe}	ε_{sbe}	ε_{dev}	A_s (dB)	$\Delta_r(\times\pi)$
B-spline	$1.009 \cdot 10^{-2}$	$1.457 \cdot 10^{-10}$	$1.457 \cdot 10^{-10}$	$1.009 \cdot 10^{-4}$	79.9	$2.485 \cdot 10^{-1}$
α-spline (C_1)	$9.732 \cdot 10^{-3}$	$1.142 \cdot 10^{-10}$	$1.142 \cdot 10^{-10}$	$8.546 \cdot 10^{-5}$	81.4	$2.394 \cdot 10^{-1}$
α-spline (C_2)	$9.802 \cdot 10^{-3}$	$6.038 \cdot 10^{-10}$	$6.038 \cdot 10^{-10}$	$9.453 \cdot 10^{-5}$	80.5	$2.493 \cdot 10^{-1}$
α-spline (C_3)	$\mathbf{9.447 \cdot 10^{-3}}$	$\mathbf{2.052 \cdot 10^{-11}}$	$\mathbf{2.052 \cdot 10^{-11}}$	$\mathbf{4.068 \cdot 10^{-5}}$	**87.8**	$2.417 \cdot 10^{-1}$
α-spline (C_4)	$1.045 \cdot 10^{-2}$	$1.123 \cdot 10^{-9}$	$1.123 \cdot 10^{-9}$	$2.570 \cdot 10^{-4}$	71.8	$2.452 \cdot 10^{-1}$

Table 3
Simulation results for different low-pass PF filters ($A_s = 60$ dB, $\omega_c = 0.25\pi$, $\Delta_r = 0.05\pi$).

Function	ε_{aisae}	ε_{pbe}	ε_{sbe}	ε_{dev}	A_s (dB)	$\Delta_r(\times\pi)$
B-spline	$2.387 \cdot 10^{-3}$	$4.696 \cdot 10^{-9}$	$4.696 \cdot 10^{-9}$	$9.984 \cdot 10^{-4}$	60.01	$4.951 \cdot 10^{-2}$
α-spline (C_1^*)	$2.146 \cdot 10^{-3}$	$3.195 \cdot 10^{-9}$	$\mathbf{3.095 \cdot 10^{-9}}$	$6.076 \cdot 10^{-4}$	64.38	$4.478 \cdot 10^{-2}$
α-spline (C_2^*)	$2.588 \cdot 10^{-3}$	$2.127 \cdot 10^{-7}$	$3.477 \cdot 10^{-7}$	$4.708 \cdot 10^{-3}$	46.15	$1.009 \cdot 10^{-1}$
α-spline (C_3^*)	$2.281 \cdot 10^{-3}$	$4.240 \cdot 10^{-8}$	$6.276 \cdot 10^{-8}$	$2.123 \cdot 10^{-3}$	53.12	$5.820 \cdot 10^{-2}$
α-spline (C_4^*)	$\mathbf{2.108 \cdot 10^{-3}}$	$\mathbf{1.303 \cdot 10^{-9}}$	$3.196 \cdot 10^{-9}$	$\mathbf{2.110 \cdot 10^{-4}}$	**72.79**	$4.584 \cdot 10^{-2}$

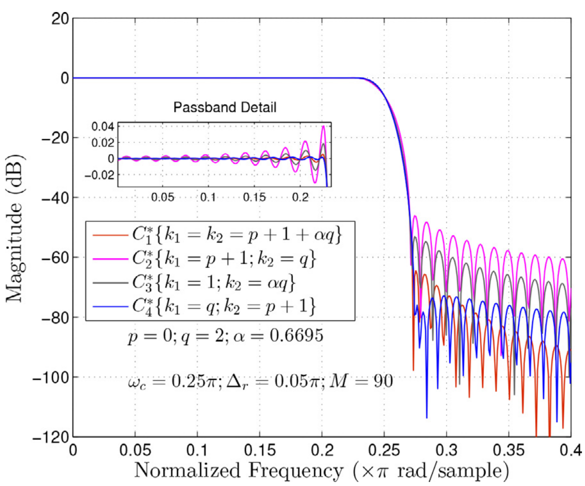

Fig. 10. Example design 2. Magnitude responses for PF low-pass $\alpha-$spline filters.

6. Conclusion

This article has presented a new parametrization of the α-spline functions on the frequency domain. Closed expressions have been derived for them, both in the frequency and time domains, and their use for digital filter design has been analysed. The continuity and differentiability properties of the frequency response have been discussed; they are inherited from the α-spline functions, and allow us to obtain both general- and special-purpose filters, the last one with special characteristics such as mainly flat filters. A method has been presented for the selection of the parameters that adjust the desired specifications and generate filters that outperform those existing in the literature. Examples of the design of mainly flat filters have been presented, and their quality has been analysed using standard metrics and compared with others obtained with different techniques. From the proposed examples, it can be inferred that it is possible to design filters with notably higher performance since the new parametrization leads to digital filters with an improvement in the stopband attenuation compared to classical methods based on B-spline. Furthermore, the new formulation also can enhance all the considered quality metrics of the resulting digital filters.

Declaration of Competing Interest

The authors declare that they have no known competing financial interests or personal relationships that could have appeared to influence the work reported in this paper.

CRediT authorship contribution statement

Miguel Ángel Raposo–Sánchez: Conceptualization, Investigation, Methodology, Software, Writing – original draft. **José Sáez–Landete:** Investigation, Software, Supervision, Validation, Writing – review & editing. **Fernando Cruz–Roldán:** Software, Supervision, Validation, Investigation, Writing – review & editing.

Data Availability

No data was used for the research described in the article.

References

[1] D. Knuth, *and METAFONT : New Directions in Typesetting*, MA: American Mathematical Soc.,and Bedford, 1979.
[2] R. Bartels, J. Beatty, B. Barsky, Splines for Use in Computer Graphics, 1987.
[3] G. Farin, Curves and Surface for Computer Aided Geometric Design: A practical Guide, MA: Academic, Boston, 1988.
[4] H.S. Hou and H.C. Andrews, Cubic spline for image interpolation and digital filtering, *IEEE Trans. Acoust., Speech, Signal Processing* ASSP-26 (1978) 508–517.
[5] M. Unser, Splines: a perfect fit for signal and image processing, IEEE Signal Process. Mag. 16 (6) (Nov. 1999) 22–38.
[6] H. Behjat, Z. Doğan, D. Van De Ville, L. Sörnmo, Domain-informed spline interpolation, IEEE Trans. Signal Process. 67 (15) (2019) 3909–3921, doi:10.1109/TSP.2019.2922154.
[7] F. Stenger, Numerical Methods Based on Sinc and Analytic Functions, 1993.
[8] H. Li, X. Qin, D. Zhao, J. Chen, P. Wang, An improved empirical mode decomposition method based on the cubic trigonometric b-spline interpolation algorithm, Appl. Math. Comput. 332 (2018) 406–419.
[9] W. Xu, S.-H. Chen, M. Wang, W. Yang, L. Wang, Eliminating the end effect of empirical mode decomposition using a cubic spline based method, Digit. Signal Process. 110 (2021) 102936.
[10] M. Duan, D. Yoon, C.E. Okwudire, A limited-preview filtered b-spline approach to tracking control - with application to vibration-induced error compensation of a 3d printer, Mechatronics 56 (2018) 287–296.
[11] R. Romagnoli, E. Garone, Steady-state input calculation for achieving a desired steady-state output of a linear systems, 2018. 10.48550/ARXIV.1804.11185
[12] R. Romagnoli, E. Garone, A general framework for approximated model stable inversion, Automatica 101 (2019) 182–189.
[13] S. Horbelt, A. Muñoz, T. Blu, M. Unser, Spline kernels for continuous-space image processing, in: 2000 IEEE International Conference on Acoustics, Speech, and Signal Processing. Proceedings (Cat. No.00CH37100), volume 4, 2000, pp. 2191–2194 vol.4.
[14] J. Ibáñez, I. Santamaría, C. Pantaleón, Parametric smoothing of spline interpolation, Proc. of IEEE International Conference on Acoustics, Speech, and Signal Processing (ICASSP '04). Montreal (Canada) II (2004) 597–600.
[15] J. Ibáñez, C. Pantaleón, J. Diez, I. Santamaría, L. Vielva, Spline pulse shaping with ISI-free and matched filter receiver, Proc. European Signal Processing Conference. Touluse (France) (2002) 1–4.
[16] I. Santamaría, J. Ibáñez, M. Lázaro, C. Pantaleón, L. Vielva, Modeling nonlinear power amplifiers in OFDM systems from subsampled data: a comparative study using real measurements, EURASIP J. Appl. Signal Process. (12) (2003) 1219–1228.
[17] E.A.B. da Silva, L. Lovisolo, A.J.S. Dutra, P.S.R. Diniz, FIR Filter design based on successive approximation of vectors, IEEE Trans. Signal Process. 62 (15) (Aug. 2014) 3833–3848.
[18] X. Huang, S. Jing, Z. Wang, Y. Xu, Y. Zheng, Closed-form FIR filter design based

on convolution window spectrum interpolation, IEEE Trans. Signal Process. 64 (5) (2016) 1173–1186, doi:10.1109/TSP.2015.2494869.
[19] M. Dedeoğlu, Y.K. Alp, O. Arikan, FIR filter design by convex optimization using directed iterative rank refinement algorithm, IEEE Trans. Signal Process. 64 (9) (2016) 2209–2219, doi:10.1109/TSP.2016.2515062.
[20] C.-C. Tseng, S.-L. Lee, Closed-form designs of digital fractional order butterworth filters using discrete transforms, Signal Process. 137 (2017) 80–97.
[21] P. Kokil, S. Jogi, C.K. Ahn, Stability analysis of digital filters subjected to interference using generalized overflow nonlinearities, Signal Process. 148 (2018) 1–8.
[22] C. Burrus, A. Soewito, R. Gopinath, Least squared error FIR filter design with transition bands, IEEE Trans. Signal Process. 40 (Jun. 1992) 1327–1340.
[23] R. Roark, M. Escabí, $B-$Spline design of maximally flat and prolate spheroidal–type FIR filters, IEEE Trans. Signal Process. 47 (3) (Mar. 1999) 701–716.
[24] F. Cruz-Roldán, P. Martín, J. Sáez-Landete, M. Blanco-Velasco, T. Saramäki, A fast windowing-based technique exploiting spline functions for designing modulated filter banks, *IEEE Transact. Circuit. Syst.-I* 56 (1) (2009) 168–178.
[25] M. Raposo-Sánchez, J. Sáez-Landete, F. Cruz-Roldán, $\alpha-$ design of finite impulse response digital filters, Signal Process. 122 (2016) 204–212.
[26] M. Raposo-Sánchez, J. Sáez-Landete, F. Cruz-Roldán, Analog and digital filters with $\alpha-$spline, Digit Signal Process. 66 (Jul. 2017) 1–9.
[27] J. Ibáñez, Polynomial techniques in signal processing: Applications to interpolation, nonlinear modeling and communications, University of Cantabria, 2004 Ph.D. thesis.